Biophysical Chemistry, 46 (1993) 273–281
Elsevier Science Publishers B.V., Amsterdam

BIOCHE 1745

End-to-end diffusion coefficients and distance distributions from fluorescence energy transfer measurements: Enhanced resolution by using multiple acceptors with different Förster distances

Badri P. Maliwal [a], Józef Kuśba [a], Wieslaw Wiczk [a,1], Michael L. Johnson [b] and Joseph R. Lakowicz [a,*]

[a] *Center for Fluorescence Spectroscopy, Department of Biological Chemistry, University of Maryland School of Medicine, 108 North Green Street, Baltimore, MD 21201 (USA)*
[b] *Department of Pharmacology, University of Virginia, Charlottesville, Virginia 22908 (USA)*

(Received 29 July 1992; accepted in revised form 13 November 1992)

Abstract

We measured distance distributions and end-to-end diffusion coefficients of donor–acceptor pairs linked by a flexible methylene chain using frequency-domain fluorescence energy transfer measurements. The donor was an indole group, and two acceptors with different Förster distances were used. The uncertainties in the recovered parameters describing the end-to-end distance distribution and diffusion coefficient were rather large when each donor–acceptor pair was analyzed separately. It was not possible to resolve distance distributions in the presence of intra-molecular diffusion when the Förster distance was comparable to the mean and half-width of the distribution. Global analysis using two acceptors dramatically improved the resolution. Surprisingly, the Förster distances need not be very different, and a 20% difference between the two R_0 values resulted in substantial improvements in resolution. Both the simulations and the experiments suggest the benefit of using global analysis with different Förster distances to obtain reliable distance distribution parameters in the presence of diffusion.

Keywords: Förster distances; Energy transfer; Diffusion; Frequency-domain fluorescence; Donor–acceptor transfer; Distance distributions

1. Introduction

There is considerable interest in the internal flexibility and conformational dynamics of complex molecules and their role in the function of biological macromolecules [1–3]. Fluorescence methods have found widespread applications in studies of conformational dynamics [4]. For instance, fluorescence anisotropy measurements have been widely used to observe internal flexibility of proteins, membranes and other biological assemblies [5]. Similarly, fluorescence resonance energy transfer (FRET) measurements have found wide ranging applications as a spectroscopic ruler due to its dependence on the dis-

* To whom correspondence should be addressed.
[1] Permanent address: Institute of Chemistry, University of Gdańsk, Gdańsk 6, Sobieskiego 18 (Poland).

tance between the donor and acceptor molecules [6–8]. In the case of a flexible molecule, however, there exists a range of distances rather than a unique distance between the fluorophores. In 1971 Cantor and Pechukas [9] suggested that it should be possible to recover the distance distribution function of a flexible molecule from the energy transfer efficiencies using multiple donor–acceptor pairs with a range of Förster distances. This has been experimentally verified in the case of a flexible methylene chain by using multiple donor–acceptors [10] and by varying the Förster distance with an external quencher [11].

In 1972, Steinberg and coworkers [12] showed that the energy transfer leads to heterogeneity in the donor decay kinetics and can be used to obtain distance distribution parameters. Their initial experiments were multi-step measurements where the distance distribution was first recovered from the intensity decay measurements carried out at high viscosity and/or low temperature in order to eliminate intramolecular diffusion. These distance distribution parameters were subsequently used to recover diffusion coefficients from decay measurements at low viscosity [13,14]. One of the reasons for such two-step measurements was the limited capabilities of flash-lamp-based time-domain instrumentation available at that time. However, it also reflects the nature of the problem. The problem of resolving multi-exponential and/or distribution functions from fluorescence measurements is of an ill-defined and complex nature [15,16]. Therefore, it is of considerable importance to devise better methods to obtain these parameters from distance distribution measurements.

One way to significantly reduce cross-correlation among the distance distribution parameters and improve their resolution is to link some of the parameters in a model-dependent way often called global analysis [17–19]. In FRET measurements of distance distributions in the presence of diffusion, the variables which can be linked are the donor lifetime, rate of diffusion, sensitized acceptor fluorescence and the Förster distance. In our earlier experiments we assessed the improved resolution which can be obtained by such global analysis. We observed moderate improvement by changing the diffusion coefficient by a factor of 50 [20] with the assumption that the distance distribution was the same at high and low viscosity. Significantly enhanced resolution was also achieved by reduction of the donor lifetime (and Förster distance) using an external quencher, followed by global analysis assuming that the distance distribution and diffusion coefficient were not affected by the quencher [21]. Similarly, in their simulation study, Beechem and Haas [22] predicted improved resolution in the distance distribution parameters by the simultaneous analysis of both donor and the sensitized acceptor fluorescence decays. However, they did not consider the possible loss in resolution due to directly excited acceptor fluorescence, which is always present in donor–acceptor systems. In this communication we assess the possible enhancement of resolution of the distance distribution parameters and the diffusion coefficient when the Förster distance is varied by the use of multiple acceptors.

2. Materials and methods

The donor fluorophore was an indole group and the acceptor was either a methoxy or nitrobenzene group. These were attached to the ends of a 12-carbon methylene chain. The synthesis and purification of the donor, myristoyl tryptamine (TMA), and the donor–acceptors, 11-*N*-(3-acetylbenzenesulfonyl)undecanoyl tryptamine (ABUT) and 11-*N*-(3-nitrobenzenesulfonyl)undecanoyl tryptamine (NBUT) are described elsewhere [10]. (The structures are given later in Fig. 4.) The measurements were performed in methanol at 20°C on a 10 GHz frequency domain instrument [23]. The methanol solutions of the donor or donor–acceptor, with optical densities near 0.10, were excited at 287 nm with vertically polarized light; the emission was observed with magic angle conditions through a 340 nm Schott interference filter.

The theory and fitting procedure have been described in considerable detail in earlier publications [20,21]. Briefly, the donor-to-acceptor probability distance distribution at the moment of

excitation ($t = 0$) is assumed to be Gaussian, described by

$$P(r) = \frac{1}{Z}\exp\left[-\frac{(r-\bar{r})^2}{2\sigma^2}\right] \quad (1)$$

where Z is the normalization factor, $\bar{r}$ is the mean distance, and the half-width (hw) of the distribution is given by $\sigma\sqrt{8\ln 2}$. The initial number $N_0^*(r)$ of the excited molecules with the donor-to-acceptor distance r is related to the total number of the excited molecules N_{t0}^* by the equation

$$N_0^* = N_{t0}^* P(r) \quad (2)$$

The donor and acceptor moieties are assumed to undergo mutual diffusion characterized by a diffusion coefficient D. According to [14], the time-dependent change in concentration, $N^*(r, t)$, of excited donor molecules with the end-to-end distance r, is described by the diffusion equation with an additional distance-dependent transfer term,

$$\frac{\partial \bar{N}^*(r,t)}{\partial t} = -\frac{1}{\tau}\left[1+\left(\frac{R_0}{r}\right)^6\right]\bar{N}^*(r,t) + \frac{1}{N_0^*(r)} \times \frac{\partial}{\partial r}\left[N_0^*(r) D \frac{\partial \bar{N}^*(r,t)}{\partial r}\right] \quad (3)$$

In this expression $\bar{N}^*(r, t) = N^*(r, t)/N_0^*(r)$ is the excitation probability normalized by the $t = 0$ distance distribution, τ is the donor fluorescence lifetime in the absence of an acceptor, and R_0 is the Förster distance for donor–acceptor energy transfer. At each distance r the rate (k_T) of donor-to-acceptor transfer is $k_T = \tau^{-1}(R_0/r)^6$ [6]. To recover the donor distribution and diffusion parameters, eq. (2) was solved with appropriate initial and boundary conditions [24]. The resulting values of $\bar{N}^*(r, t)$ were used to compute the donor intensities by the relation

$$I(t) = I_0 \int_{r_{min}}^{r_{max}} P(r)\bar{N}^*(r,t)\,dr \quad (4)$$

where r_{min} and r_{max} are minimal and maximal donor-to-acceptor distances. The data were also fit to a multi-exponential decay

$$I(t) = I_0 \sum_i \alpha_i \exp(-t/\tau_i) \quad (5)$$

where α_i are the pre-exponential factors, $\Sigma\alpha_i = 1.0$, and τ_i the decay times. The fractional intensity (f_i) of each component in the decay is given by $f_i = \alpha_i\tau_i/\Sigma_j\alpha_j\tau_j$. The mean decay time $\langle\tau\rangle = \Sigma_i f_i\tau_i$.

The goodness-of-fit is characterized by

$$\chi_R^2 = \frac{1}{\nu}\sum_\omega\left[\frac{\phi_\omega - \phi_{c\omega}}{\delta\phi}\right]^2 + \frac{1}{\nu}\sum_\omega\left[\frac{m_\omega - m_{c\omega}}{\delta m}\right]^2 \quad (6)$$

where ν is the number of degrees of freedom, and $\delta\phi$ and δm are the experimental uncertainties in the measured phase angles (ϕ_ω) and modulation (m_ω), respectively. These uncertainties were taken to be $\delta\phi = 0.2°$ and $\delta m = 0.005$ [25]. In some of the global analyses, results from an earlier publication for same donor and linker but different acceptor (and different R_0) were used [24].

3. Analysis of simulated data

For simulations, data files were created consisting of about 22 frequencies which cover modulations from 0.99 to 0.20. Random (Gaussian) noise was added at the level of 0.2° in the phase and 0.005 in the modulation [25]. The parameters used in the simulations were a 5 ns donor lifetime, a mean distance ($\bar{r}$) and a half-width (hw) of 20 Å, and an end-to-end diffusion coefficient of 5×10^{-6} cm^2/s. The Förster distances (R_0) were varied between 20 Å and 32 Å. To account for correlations between the parameters ($\bar{r}$, hw, and D), χ_R^2 surfaces were created by fixing one parameter to a given value and allowing the other two parameters to vary during the fitting procedure. To eliminate statistical anomalies in the simulated files, the data for each set of parameters were calculated twice, each time with new values of random noise. For global analysis four

pairs of simulated files were analyzed separately, where one file had $R_0/\bar{r} = 1$ and the second file was for $R_0/\bar{r} = 1.05$, 1.10, 1.15, or 1.20.

Figure 1 shows some representative χ^2_R surfaces for the diffusion coefficient (D) as a function of $R_0/\bar{r}$. The solid lines represent non-global analyses for a single R_0 value. The dotted line indicates the 95% confidence limit. The χ^2_R surfaces are bell shaped and the confidence intervals become smaller as the Förster distance is increased. It is clear from Fig. 1 that when the R_0, $\bar{r}$ and hw are similar ($R_0/\bar{r} = 1$), it would be difficult to determine the true value of D (bottom solid line). For clarity, in all representations, we averaged the lower and upper limits of the confidence intervals and expressed these values as the percent of the mean value. Since the χ^2_R surfaces have nearly symmetrical shapes, it seems reasonable to average the confidence interval limits. Such averaged confidence interval limits in the case of D as a function of $R_0/\bar{r}$ are shown in Fig. 2A. The improvement in the resolution of D as a function of $R_0/\bar{r}$ is now more obvious. However, even at the highest value of R_0 ($R_0/\bar{r} = 1.6$) where the extent of the energy transfer is about 90% (Fig. 2B), the uncertainties in D are still almost 50% of the mean and may be considered unsatisfactory.

A representative χ^2_R surface from global analysis involving simulated data for $R_0/\bar{r}$ of 1 and 1.2 (— — —) is also shown in Fig. 1. A dramatic

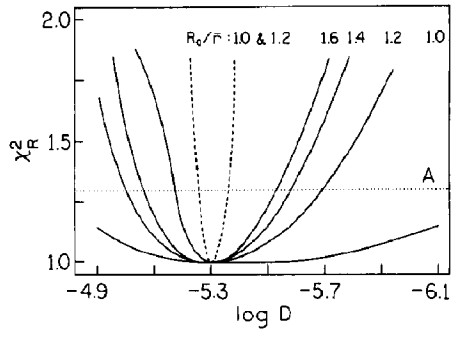

Fig. 1. χ^2_R surfaces for the diffusion coefficient (D) at various values of the $R_0/\bar{r}$. The dotted line represents the 95% confidence limit. The dashed line represents a two-file global analysis. The data were simulated using $\bar{r} = hw = 20$ Å, $D = 5 \times 10^{-6}$ cm^2/s.

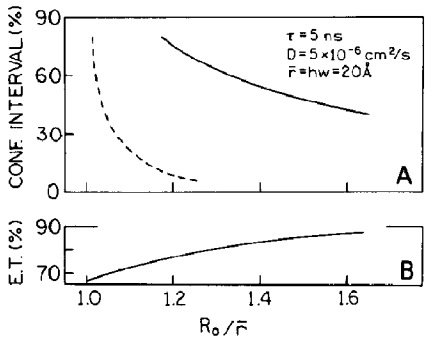

Fig. 2. (A) Confidence intervals for D at different $R_0/\bar{r}$ values for global (— — —) and single file (———) analysis. (B) Energy transfer efficiencies for different $R_0/\bar{r}$ values.

improvement is seen in the confidence limits when compared to single R_0 files. A similar global analysis was also performed for $R_0/\bar{r}$ pairs: 1 and 1.05; 1 and 1.10; and 1 and 1.15. These results are shown as the dashed line in Fig. 2A. The uncertainties in D in the global analysis also decrease as R_0 for the second file is increased. However, when compared with non-global analysis, the slope is sharper for global analysis. For example a global analysis using only two files, $R_0/\bar{r} = 1$ and 1.2, is adequate for recovering the diffusion coefficient with an uncertainty of less than 10%. To show that the simulations were carried out for experimentally feasible situations, the energy transfer efficiencies as a function of $R_0/\bar{r}$ are shown in Fig. 2B. The maximum value for energy transfer in the simulations is about 90% for the case of $R_0/\bar{r} = 1.6$. This system would be considered experimentally feasible if the donor quantum yield is good.

Figure 3 shows the confidence interval limits, expressed as a percent of the mean, for hw and $\bar{r}$ as a function of $R_0/\bar{r}$. The solid lines are the results from non-global analysis of single R_0 files while that from global analysis are given as dashed lines. Again the parameters are poorly resolved at $R_0/\bar{r} = 1$, and the uncertainties decrease as the ratio of $R_0/\bar{r}$ is increased in single R_0 analysis. Also, the uncertainties are relatively lower in the case of $\bar{r}$ when compared with hw (Fig. 3) and D (Fig. 2A). When compared to single R_0 analysis, a significant improvement is obvious with

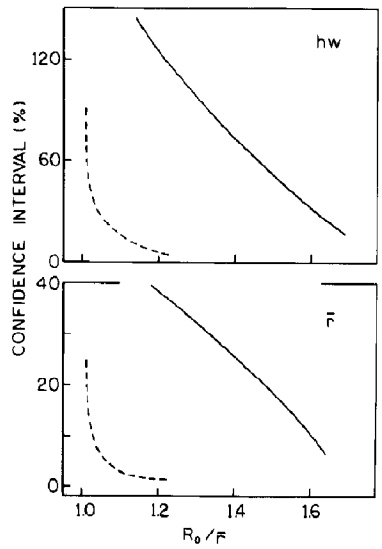

Fig. 3. Confidence intervals for *hw* (top) and $\bar{r}$ (bottom) as a function of $R_0/\bar{r}$ in the case of global (— — —) and single file (———) analysis. These are the same simulated data sets as in Fig. 1.

global analysis. A global analysis involving even the closest of two R_0 values (1 and 1.05) gives resolution comparable to that of single file analysis with $R_0/\bar{r} = 1.6$. The uncertainties are less than 10% when the two files for $R_0/\bar{r} = 1$ and 1.2 are simultaneously analyzed.

To summarize, these simulations suggest that in the presence of diffusion, $\bar{r}$ and *hw* will be poorly resolved if the values of R_0 and $\bar{r}$ are similar. A dramatic improvement in the resolution can, however, be obtained if a second measurement involving a different Förster distance is also carried out. Furthermore, this second R_0 need not be significantly different from the first R_0. It should be noted that the enhanced resolution obtained with the second R_0 file (Figs. 2 and 3) is valid for these specific values of $\bar{r}$, *hw*, and *D*. For example, conditions such as a lower value of hw and higher value of *D*, which would decrease the extent of heterogeneity in the donor decays, will also make resolution of the parameters more difficult.

4. Experimental results

Fluorescence emission spectra of the donor (TMA) and two donor–acceptor pairs (ABUT) and NBUT) in methanol at 20°C are shown in Fig. 4. There is considerable energy transfer ($\geq$ 80%) to both acceptors. The multi-exponential analysis of donor–acceptor intensity decays are given in Table 1. The donor fluorescence is characterized by a lifetime of 4.66 ± 0.05 ns. Energy transfer to the acceptor significantly reduces the lifetime of the indole fluorophore in both ABUT and NBUT. It also results in a heterogenous decay as seen by the χ^2_R values for the single exponential (1τ) fits (Table 1). The heterogeneity, though modest, increases with increased energy

Table 1

Multicomponent analysis of frequency-domain intensity decays of the donor emission in methanol at 20°C [a]

Compound	$\langle\tau\rangle$ [b] (ns)	1 τ [c]		2 τ [c]		χ^2_R	
		τ_i (ns)	f_i	τ_i (ns)	f_i	1 τ [c]	2 τ [c]
TMA	4.66	4.66	1.00	–	–	1.31	–
ABUT	0.90	0.88	1.00	0.29	0.04	6.82	0.80
				0.92	0.96		
NBUT	0.59	0.57	1.00	0.18	0.07	20.33	1.33
				0.62	0.93		
TUD [d]	0.47	0.35	1.00	0.11	0.20	491.0	3.90
				0.57	0.80		

[a] The excitation wavelength was 287 nm and the emission was observed through a Schott 340 nm interference filter. The error levels of 0.2° (phase) and 0.005 (modulation) are assumed for analysis.

[b] $\langle\tau\rangle$ is the average lifetime value.

[c] 1 τ and 2 τ refers to single and double exponential fits, respectively.

[d] From ref. [24]. The TUD sample was deoxygenated, and had a donor lifetime of 5.7 ns.

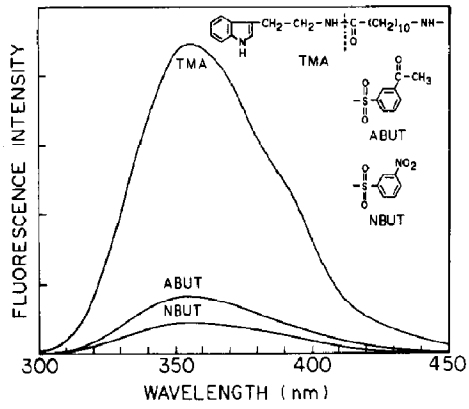

Fig. 4. Fluorescence emission spectra of the donor (TMA) and donor–acceptor pairs (ABUT and NBUT) in methanol at 20°C. The excitation was 290 nm and slit widths of 8 nm were used. TMA is the amide conjugate of tryptamine with myristic acid ($CH_3(CH_2)_{12}CO_2H$).

transfer as seen by value of χ^2_R of 20.3 for NBUT ($\langle\tau\rangle = 0.59$) as compared to 6.8 for ABUT ($\langle\tau\rangle = 0.90$). Also included in Table 1 are results for dansyl undecanoyl tryptamine (TUD) which are from an earlier publication [24]. Both the energy transfer and the extent of heterogeneity are greater in the case of TUD as compared to other two acceptors.

The χ^2_R surfaces for distance distribution analysis which include intramolecular diffusion, in the case of ABUT and NBUT, are shown in Figs. 5 and 6 by solid lines. We could not obtain reasonable confidence limits from the single file analysis for either ABUT or NBUT, as can be seen from the χ^2_R surfaces (Figs. 5 and 6, solid line). This is also evident from the modest increases in χ^2_R when diffusion is eliminated (diffusion coefficient is fixed at 1×10^{-5} cm^2/s) or when the half-width is set to a narrow value of 3 Å (Table 2). Clearly, by themselves, these fluorescence decays cannot provide a satisfactory resolution of $\bar{r}$, *hw* and *D*. Also given in Table 2 are the results of distance distribution analysis for TUD from an earlier publication [24]. The R_0 for this donor–acceptor (24.8 Å) is substantially larger than that for ABUT and NBUT (10.2 Å and 13.7 Å). For this higher R_0 value donor–acceptor pair, we were able to recover $\bar{r}$, *hw* and *D* without the use of global analysis, although with modestly large uncertainties (Table 2).

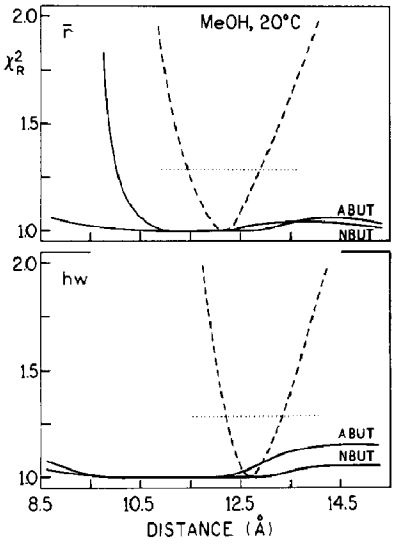

Fig. 5. χ^2_R surfaces for $\bar{r}$ and *hw* generated from single file (———) and global analysis (— — —) of ABUT and NBUT frequency-domain data. The dotted line represents the 95% confidence limit.

The results from global analysis for ABUT and NBUT are also given in Table 2, and the χ^2_R surfaces (dashed line) are shown in Fig. 5 ($\bar{r}$, *hw*), in Fig. 6 (*D*), and the fit to donor intensity decays in Fig. 7. A dramatic improvement in resolution is seen for global analysis when compared to separate analysis. The confidence intervals are now about 5 to 10% of the mean in the case of $\bar{r}$

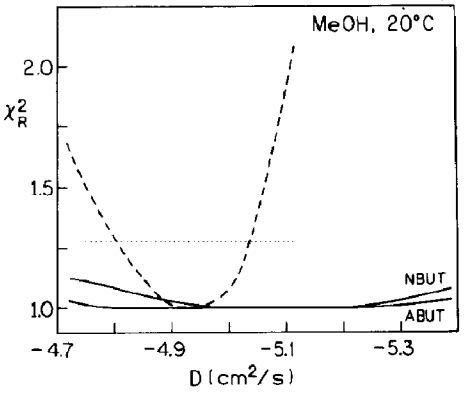

Fig. 6. χ^2_R surfaces for the diffusion coefficient generated from single file (———) and global analysis (— — —) for ABUT and NBUT. The dotted line represents the 95% confidence limit.

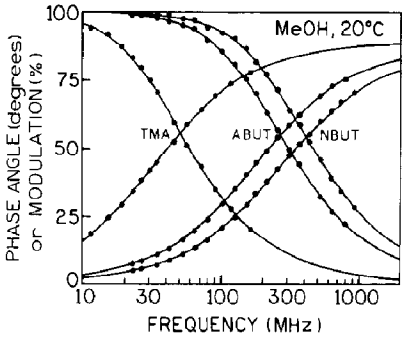

Fig. 7. Global distance distribution fits to frequency-dependent phase angles and modulations for ABUT and NBUT. The recovered parameters are $\bar{r} = 12.1$ Å, $hw = 12.7$Å, $D = 1.15 \times 10^{-5}$ cm^2/s, and χ^2_R value of 1.42. The TMA data are fit with a single-exponential lifetime model.

and hw and less than 30% for the diffusion coefficient. A similar improvement in resolution is observed from global analysis of NBUT and TUD (Table 2). Furthermore, we were able to satisfactorily resolve two end-to-end diffusion coefficients in the case of NBUT and TUD. A slower end-to-end diffusion coefficient is expected in the case of TUD as the dansyl moiety is bulkier when compared to the substituted benzene group in ABUT and NBUT. Furthermore, as expected the presence of two end-to-end diffusion coefficients also results in somewhat larger uncertainties in the hw value. The resolution of the parameters is somewhat better when ABUT, NBUT and TUD are globally analyzed. However, a comparison of the uncertainties between the NBUT and TUD global analysis and global analysis including ABUT, NBUT and TUD suggests only a marginal improvement is obtained upon adding a third acceptor. The recovered parameters ($\bar{r}$, hw, and D) are quite similar in all three global analyses.

Table 2

Distance distribution parameters and diffusion coefficients for ABUT, NBUT and TUD

Compound	R_0 (Å)	$\bar{r}$ (Å)	hw (Å)	D (cm^2/s)	χ^2_R
ABUT [a]	10.2	12.0	11.1	10×10^{-6}	1.45
		8.0	0.6	$\langle 1 \times 10^{-15} \rangle$ [b]	3.22
		8.3	⟨3.0⟩	5.2×10^{-7}	1.70
NBUT [a]	13.7	11.6	11.4	9×10^{-6}	1.22
		9.8	1.1	$\langle 1 \times 10^{-15} \rangle$	4.03
		9.9	⟨3.0⟩	3.7×10^{-7}	1.79
TUD [c]	24.8	12.2	13.0	2.5×10^{-6}	2.30
		(8.4–13.6) [d]	(8.0–18.0)	(5.2–0.6)	
NBUT and ABUT		12.1	12.7	11.5×10^{-6}	1.42
		(11.4–12.9)	(12.2–13.3)	(15.6–9.2)	
NBUT and TUD		12.1	13.2	12.4×10^{-6}	1.66
		(11.4–12.6)	(11.9–14.5)	(11.1–13.8)	
				2.6×10^{-6}	
				(2.0–3.4)	
ABUT and NBUT and TUD		12.2	12.8	12.3×10^{-6}	1.64
		(11.8–12.6)	(11.5–13.8)	(10.8–14.6)	
				12.4×10^{-6}	
				(11.1–13.7)	
				2.5×10^{-6}	
				(2.0–3.1)	

[a] Confidence intervals cannot be determined at a 95% confidence limit.

[b] ⟨·⟩ Indicates the parameter value was held fixed at the indicated value.

[c] From ref. [24].

[d] Values in parentheses indicate 95% confidence interval.

5. Discussion

The simulations and experimental results both indicate that it is generally difficult to recover $\bar{r}$ and hw in the presence of end-to-end diffusion. However, when R_0 is greater than $\bar{r}$, then both simulations and experiments (TUD, [24]) indicate that it should be possible to recover all three parameters ($\bar{r}$, hw and D) though with significant uncertainties. A dramatic improvement in resolution of the distance distribution parameters and the diffusion coefficient, however can be observed with the use of two Förster distances. It is not clear why the resolution dramatically improved in the global analysis even when two R_0 values differed by only 10%. However, such a 10% difference in R_0 can have a substantial effect on the decay of the donor, and thereby alter the information content of the donor data in the presence of each of the acceptors. Global analysis of these sets of data then allows improved resolution of the distance distribution and diffusive contributions to the donor decay.

Even though the global analysis using two R_0 values leads to a dramatic improvement in the resolution, the introduction of a second donor or acceptor to vary the Förster distance involves additional chemical synthesis. However, this should not be limiting because in the case of macromolecules, a fluorophore is often reacted to a specific group, and several different fluorophores with the same reactive group are commercially available. Another possible approach is to vary the Förster distance (and donor lifetime) using an external quencher [21]. This procedure avoids the need for additional chemical synthesis. However, the extent of change in R_0 which can be obtained by the external quencher is limited due to the inverse sixth power dependence of R_0 on the quantum yield [6]. Also, there are practical limits to the extent of quenching especially for fluorophores with low quantum yields.

Most of the reported distance distributions [12–14,22] have assumed Gaussian functions which are easy to use in the computer algorithm. In the case of oligomers, both theory [26] and experiments [10,27] suggest that the distribution is non-Gaussian and skewed towards shorter distances. Similarly, as biological systems are inherently complex, their conformational distributions are also more likely to be asymmetrical. Therefore it is important to be able to resolve skewed Gaussian distributions satisfactorily. However, introduction of a skew in the distribution appears to increase the correlation among the parameters. In experiments where intramolecular diffusion was minimized with high viscosity and 13 acceptors with different Förster distances were used, both steady-state measurements [10] and frequency-domain measurements [27] showed a modest difference between Gaussian and skewed-Gaussian fits. The uncertainties in the recovered skewed distribution parameters were also considerable. When end-to-end diffusion was also included along with the skewed distribution, the differences between the models became even smaller, and the uncertainties larger (unpublished simulations). These results are somewhat discouraging and suggest the need for further improvements. As the correlations are different for each linkage, perhaps a global approach which will simultaneously use linkages involving Förster distance, sensitized emission and donor lifetimes may help resolve the more complex distributions. Also encouraging in this regard is the continuous improvement in the frequency-domain instrumentation. For example, enhanced resolution can be expected due to superior signal-to-noise using digital data acquisition [28], and methods for parallel data acquisition [29] may allow the practical utilization of acceptor decay data. Similarly, the extension of the time-resolution to the subpicosecond timescale [23,30,31] should also improve the resolution, as the differences among different models are manifested primarily at the very early times of the fluorescence decays.

Acknowledgments

The authors acknowledge support from the National Institutes of Health, (GM35154), with support for instrumentation and the Center for Fluorescence Spectroscopy, and the National Science Foundation (DIR-8710401 and DMB-8804931). JRL and WW also express appreciation

for support from the Medical Biotechnology Center at the University of Maryland.

References

1 M. Karplus and J. A. McCammon, CRC Crit. Rev. Biochem. 9 (1981) 292.
2 J.A. McCammon and S.C. Harvey, Dynamics of proteins and nucleic acid (Cambridge University Press, New York, 1987).
3 G.R. Welch, Fluctuating enzyme (Wiley, New York, 1986).
4 A.P. Demchenko, in: Topics in fluorescence spectroscopy, vol. 3, ed. J.R. Lakowicz (Plenum Press, New York, 1992) p. 1.
5 R.F. Steiner, in: Topics in fluorescence spectroscopy, vol. 2, ed. J.R. Lakowicz (Plenum Press, New York, 1991) p. 1.
6 T. Förster, Ann. Phys. (Leipzig) 2 (1948) 55.
7 L. Stryer, Annu. Rev. Biochem. 47 (1978) 819.
8 T.G. Dewey, in: Biophysical and biochemical aspects of fluorescence spectroscopy, ed. T.G. Dewey (Plenum Press, New York, 1991) p. 197.
9 C.R. Cantor and P. Pechukas, Proc. Natl. Acad. Sci. (USA) 68 (1971) 2099.
10 W. Wiczk, P.S. Eis, M.N. Fishman, M.L. Johnson and J.R. Lakowicz, J. Fluorescence 1 (1992) 273.
11 I. Gryczynski, W. Wiczk, M.L. Johnson, H.C. Cheung, C.-K. Wang and J.R. Lakowicz, Biophys. J. 54 (1988) 577.
12 A. Grinvald, E. Haas and I.Z. Steinberg, Proc. Natl. Acad. Sci. (USA) 69 (1972) 2273.
13 E. Haas, M. Wilchek, E. Katchalski-Katzir and I.Z. Steinberg, Proc. Natl. Acad. Sci. (USA) 72 (1975) 1807.
14 E. Haas, E. Katchalski-Katzir and I.Z. Steinberg, Biopolymers, 17 (1978) 11.
15 C. Lanczos, Applied analysis (Prentice Hall, Inglewood Cliffs, NJ, 1956).
16 M.L. Johnson, Biophys. J. 44 (1983) 101.
17 M.L. Johnson, H.R. Halvorson and G.K. Ackers, Biochemistry, 15 (1976) 5563.
18 J.R. Knutson, J.M. Beechem and L. Brand, Chem. Phys. Lett. 102 (1983) 501.
19 J.M. Beechem, M. Ameloot and L. Brand, Anal. Instrum. 14 (1985) 379.
20 J.R. Lakowicz, J. Kuśba, W. Wiczk, I. Gryczynski and M.L. Johnson, Chem. Phys. Lett. 173 (1990) 319.
21 J.R. Lakowicz, J. Kuśba, I. Gryczynski, H. Szmacinski and M.L. Johnson, J. Phys. Chem. 95 (1991) 9654.
22 J.M. Beechem and E. Haas, Biophys. J. 55 (1989) 1225.
23 G. Laczko, I. Gryczynski, H. Szmacinski, W. Wiczk, H. Malak and J.R. Lakowicz, Rev. Sci. Instrum. 61 (1990) 2331.
24 J.R. Lakowicz, J. Kuśba, W. Wiczk, I. Gryczynski, H. Szmacinski, and M.L. Johnson, Biophys. Chem. 39 (1991) 79.
25 J.R. Lakowicz, G. Laczko, H. Cherek, E. Gratton and M. Limkeman, Biophys. J. 46 (1984) 463.
26 P. Flory, Statistical mechanics of a chain molecule, (Wiley, New York, 1969).
27 M.N. Fishman, P.S. Eis, W. Wiczk and J.R. Lakowicz, Biophys. J. 59 (1991) 354a.
28 B.A. Feddersen, D.W. Piston and E. Gratton, Rev. Sci. Instrum. 60 (1989) 2929.
29 E. Gratton, B. Feddersen and M. vandeVen, Proc. SPIE 1204 (1990) 21.
30 K. Berland, M. Dowling, M. vandeVen and E. Gratton, Biophys. J. 59 (1991) 167a.
31 J.E. Hansen, S.J. Rosenthal and G.R. Fleming, J. Phys. Chem. 96 (1992) 3034.